THE ASTRONOMICAL JOURNAL, 117:1700–1707, 1999 April

DEEP *HUBBLE SPACE TELESCOPE* OBSERVATIONS OF BLUE STAR CLUSTERS IN NGC 3597[1]

MATTHEW N. CARLSON,[2] JON A. HOLTZMAN,[2] CARL J. GRILLMAIR,[3] JEREMY R. MOULD,[4] RICHARD E. GRIFFITHS,[5] GILDA E. BALLESTER,[6] CHRISTOPHER J. BURROWS,[7] JOHN T. CLARKE,[6] DAVID CRISP,[8] ROBIN W. EVANS,[8] JOHN S. GALLAGHER III,[9] J. JEFF HESTER,[10] JOHN G. HOESSEL,[9] PAUL A. SCOWEN,[10] KARL R. STAPELFELDT,[8] JOHN T. TRAUGER,[8] ALAN M. WATSON,[11] AND JAMES A. WESTPHAL[12]

Received 1998 December 1; accepted 1999 January 12

ABSTRACT

We have analyzed *HST*/WFPC2 images of NGC 3597 and find ~700 compact objects surrounding the galaxy with an average $(B-R)_0 \sim 0.6$. We propose that the majority of these objects are young globular clusters. They have a spread in colors that is consistent with that expected for a population of young clusters with a common age and spread induced by photometric errors and reddening within NGC 3597. If these objects were similar to the Galactic globular cluster system seen at a younger age, we would predict a turnover in the luminosity function at $B \sim 23$. However, we find that the luminosity function for the clusters is increasing to the limits of our photometry ($B \sim 27$).

Key words: galaxies: star clusters

1. INTRODUCTION

NGC 3597 is an isolated galaxy, yet it has a disturbed morphology. Its surface brightness profile is well fitted by a de Vaucouleurs law, which is characteristic of elliptical galaxies. However, the galaxy is also undergoing intense star formation. Lutz (1991) noted that there are three diffuse plumes in the western region of the galaxy. This evidence suggests that NGC 3597 underwent a merger $\lesssim 1$ Gyr ago.

Lutz (1991) found a population of 14 blue ($B-V < 1$) objects in NGC 3597, which he proposed were young globular clusters. However, his ground-based data did not have the resolution to say definitively whether they were as compact as globular clusters or not. A later study by Holtzman et al. (1996) based on *Hubble Space Telescope* (*HST*) data detected 72 potential clusters, which were found to be comparable in size to globular clusters and which had inferred ages of $\lesssim 500$ Myr. The brightest object has $V = 20.3$, which corresponds to $M_V = -13.3$ for a distance modulus of 33.6 ($H_0 = 75$ km s^{-1} Mpc^{-1} and $cz = 3513$ km s^{-1}) (de Vaucouleurs et al. 1991, Vol. 2, p. 262). This magnitude corresponds to a mass of $\sim 10^7\ M_\odot$, depending on the age, distance, and metallicity, and assuming a Salpeter IMF.

Young clusters have been detected in a variety of galaxies, including dwarf galaxies, ring galaxies, starbursts, and interacting galaxies. While no single unifying picture has emerged to explain all incidences of young clusters, it is clear that galaxy interaction likely plays a role in their formation. As these clusters are observed in recently merged galaxies, they may shed some light on the question of whether elliptical galaxies can form from the merger of spiral galaxies and if the specific frequency can increase in such a merger (see Ashman & Zepf 1992).

Despite much interest in the field of young globulars, relatively few of the young cluster systems have well-measured luminosity functions. Many of the galaxies with young clusters have only a few clusters, which gives little information about the luminosity function of these objects. Other systems have not been observed to faint enough magnitudes to detect large numbers of clusters. To date, well-measured luminosity functions exist for NGC 4038/9 (Whitmore & Schweizer 1995), NGC 3921 (Schweizer et al. 1996), NGC 7252 (Miller et al. 1997), NGC 1275 (Carlson et al. 1998), and NGC 3256 (Zepf et al. 1999). In all of these galaxies, the luminosity function of the young clusters has been found to be increasing to the limits of the photometry, in contrast to the Galactic globular cluster luminosity function, which is roughly Gaussian with a turnover at $M_B = -6.6$.

We have obtained WFPC2 images of NGC 3597 that go ~2 mag deeper in R than the WFPC2 images of Holtzman et al. (1996). If the luminosity function of these young globu-

[1] Based on observations with the NASA/ESA *Hubble Space Telescope*, obtained at the Space Telescope Science Institute, operated by AURA, Inc. under contract to NASA.

[2] Department of Astronomy, New Mexico State University, Department 4500, Box 30001, Las Cruces, NM 88003; mcarlson@nmsu.edu, holtz@nmsu.edu.

[3] SIRTF Science Center, M/S 100-22, California Institute of Technology, 770 South Wilson, Pasadena, CA 91125; carl@bugaboo.ipac.caltech.edu.

[4] Mount Stromlo and Siding Spring Observatories, Australian National University, Private Bag, Weston Creek Post Office, ACT 2611, Australia; jrm@mso.anu.edu.au.

[5] Department of Physics, Carnegie Mellon University, 5000 Forbes Avenue, Pittsburgh, PA 15213.

[6] Department of Atmospheric, Oceanic, and Space Sciences, University of Michigan, 2455 Hayward, Ann Arbor, MI 48109; gilda@sunshine.sprl.umich.edu, clarke@sunshine.sprl.umich.edu.

[7] Astrophysics Division, Space Science Department, ESA; and Space Telescope Science Institute, 3700 San Martin Drive, Baltimore, MD 21218; burrows@stsci.edu.

[8] Jet Propulsion Laboratory, 4800 Oak Grove Drive, Pasadena, CA 91109; dc@crispy.jpl.nasa.gov, rwe@wfpc2-mail.jpl.nasa.gov, krs@wfpc2-mail.jpl.nasa.gov, jtt@wfpc2-mail.jpl.nasa.gov.

[9] Department of Astronomy, University of Wisconsin–Madison, 475 North Charter Street, Madison, WI 53706; jsg@tiger.astro.wisc.edu, hoessel@jth.astro.wisc.edu.

[10] Department of Physics and Astronomy, Arizona State University, Tyler Mall, Tempe, AZ 85287; jjh@cosmos.la.asu.edu, scowen@tycho.la.asu.edu.

[11] Instituto de Astronomía, Universidad Nacional Autónoma de México, J. J. Tablada 1006, Col. Lomas de Santa Maria, 58090 Morelia, Michoacán, Mexico; alan@astrosmo.unam.mx.

[12] Division of Geological and Planetary Sciences, California Institute of Technology, Pasadena, CA 91125; jaw@sol1.gps.caltech.edu.

lars after 13 Gyr of fading will come to resemble the lognormal luminosity function of the Galactic globular cluster system, we can predict, based on stellar evolution models, what the present-day magnitude of the turnover in the luminosity function of these clusters would be. Our current observations probe ~ 4 mag beyond this predicted turnover if these objects are younger analogs of Galactic globular clusters.

Section 2 presents a brief summary of the observations and data reduction. Section 3 discusses our photometry technique, completeness strategy, and potential errors. Section 4 details the results of our photometry, the luminosity function of the blue clusters, the surface density profile, and the distribution of cluster sizes and presents a discussion of the specific frequency.

2. OBSERVATIONS AND DATA REDUCTION

NGC 3597 was observed with the WFPC2 on 1997 May 16 in the F450W and F702W filters. In the F450W filter, we took four exposures of 1300 s each. In the F702W filter, exposure times were 1100 and 3×1300 s. The F450W and F702W filters are comparable to broadband B and R filters.

The data were reduced using the procedures of Holtzman et al. (1995a). Hot pixel subtractions were done using dark frames taken within 2 weeks of the object exposures to correct the hot pixels, which are variable in time; higher signal-to-noise ratio dark frames from several months of dark exposures were used for all other pixels. The individual exposures were taken with a common pointing, and the frames in each filter were averaged. Cosmic rays were rejected during this combination by rejecting pixels that deviated by an amount significantly larger than that expected based on the expected variance from photon statistics and readout noise; an extra term was included in the expected variance that was proportional to the signal in the pixel to allow for small pointing differences between frames.

Our faintest detections may be slightly contaminated by the presence of hot pixels. However, we estimate that the hot pixels contribute $<9\%$ of the detections in the PC in the range $B = 26.5$–28, with negligible numbers of hot pixel detections at brighter magnitudes. This estimate is based on coincidences of detected objects with hot pixels from dark frames taken 7 days after the observations. This potential minor contamination does not significantly alter the conclusions of this paper. We note that these observations took place 1 day after a monthly decontamination of the chip.

3. ANALYSIS

We present a combined color image of NGC 3597 in the PC frame in Figure 1. The image is centered on the central region of NGC 3597. Almost all of the visible point sources are young cluster candidates, although there are a few sources that may be foreground stars or members of the old globular cluster systems of the progenitors of NGC 3597. Based on the stellar distribution models of Bahcall & Soneira (1980), we predict approximately less than two foreground stars in the PC field of view for $B < 27$ and approximately six in each of the WFs.

To aid in finding objects against the background light from the galaxy, we subtracted a 5×5 boxcar-smoothed version of the image. We divided the resultant image by the square root of the smoothed image to provide a uniform detection threshold in signal-to-noise ratio across the image. We determined an appropriate detection level by visual inspection, attempting to minimize spurious detections and maximize the detection of real objects. Finally, we rejected all objects in three masks near the galaxy center that suffered from wildly varying background levels, which made accurate photometry impossible.

Photometry of the clusters in NGC 3597 was performed with IRAF's DAOPHOT. To measure magnitudes in the PC, where most of the blue clusters were located, we used an aperture with a radius of 2 pixels centroided on each source. To determine the sky level, we took the mode of the values in an annulus from 12 to 14 pixels wide. Selecting an aperture correction to correct to the standard radius of 0.″5 (Holtzman et al. 1995b) for our measured magnitudes was complicated by the fact that these objects appear to be slightly resolved with significant scatter in their sizes. To attempt to correct for this, we used the observation that the aperture correction was correlated with $m_1 - m_2$, the difference between the magnitude measured in 1 and 2 pixel apertures. We measured these quantities for 23 of the brightest clusters (there was no correlation between total magnitude and aperture correction). This is displayed in Figure 2 for our measurements in B and R. Also shown in the plot are the adopted linear fits to the data. We then measured the 1 to 2 pixel aperture magnitude difference for all objects with $B < 26.5$ and applied the appropriate aperture correction based on our fits to the bright clusters. For objects with aperture corrections outside the range of our bright clusters, $m_1 - m_2 = 0.7$–0.9, we used the closest correction within our range (i.e., for clusters with $m_1 - m_2 < 0.7$, we used the correction for 0.7). We chose a magnitude cutoff of $B = 26.5$ to avoid giving inaccurate aperture corrections to objects with relatively large errors in $m_1 - m_2$. For those objects fainter than our adopted cutoff, we assumed a constant aperture correction, which was the mean of the measured aperture corrections of the bright objects (0.57 and 0.64 mag in B and R, respectively).

In the WFs, we performed photometry with a 2 pixel aperture and a sky annulus with an inner radius of 8 pixels and an outer radius of 11 pixels. We used a constant aperture correction in the WFs, as variation in individual aperture corrections is less important because of the decreased resolution. For the aperture corrections, we took the average of several relatively bright isolated sources. In B, we determined a correction from 2 pixels to 0.″5 of 0.19 mag, while in R the correction was 0.20 mag.

In the PC, completeness was determined by placing 1000 artificial clusters with $B-R = 0.7$ in each of three annuli surrounding the nucleus (100–200, 200–350, and >350 pixels). As a template for the PSF, we used a single bright isolated cluster. To alleviate the problem of varying sizes of the clusters as much as possible, we chose a cluster with an average value of $m_1 - m_2$. The artificial clusters were placed with the same radial distribution as the bright clusters ($B < 26$) within each annulus. These artificial cluster images were processed in exactly the same manner as the original photometry. To determine the overall completeness as a function of magnitude, we measured the percentage of artificial clusters detected in each annulus and weighted this by the actual number of bright clusters in each of the three annuli. This is shown in Figure 3. No attempt was made to determine completeness in the WFs, owing to the potentially large fraction of the sources that are unrelated to the blue clusters.

FIG. 1.—PC image of NGC 3597

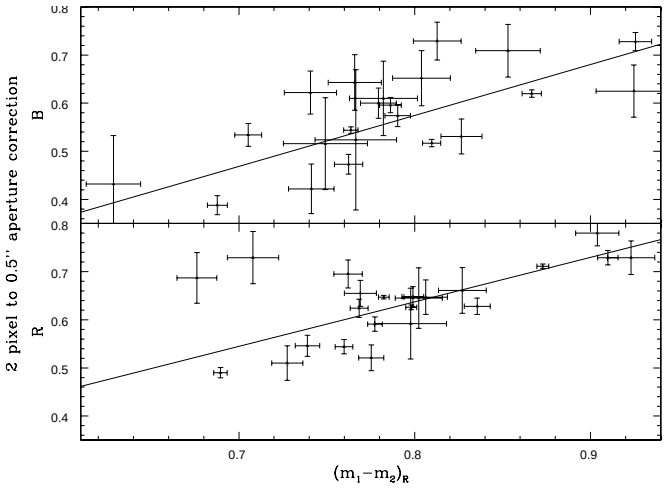

FIG. 2.—Aperture correction plotted vs. 1 to 2 pixel aperture magnitude difference for B and R. The points are from the 23 brightest clusters.

Completeness varies somewhat with color, but this does not affect the conclusions of this paper to any great extent. Even for objects one-half magnitude bluer ($B-R=0.2$), our completeness is still over 90% for $B<25.5$, the magnitude region upon which we base most of our conclusions. Objects with colors redder than 0.7 are more complete than our models, owing to the higher signal to noise in the F702W images.

The errors in our photometry come from Poisson error in the signal, error in the sky background, and errors in both the measured aperture correction and the assumed linear relationship between m_1-m_2 and the aperture correction. To estimate errors in our measured magnitudes, we plot the output magnitudes and colors of a randomly selected subsample of the artificial clusters from our completeness tests. We chose numbers of clusters from each annulus that were proportional to the measured numbers of bright clusters in each annulus. Figure 4 shows the output colors plotted

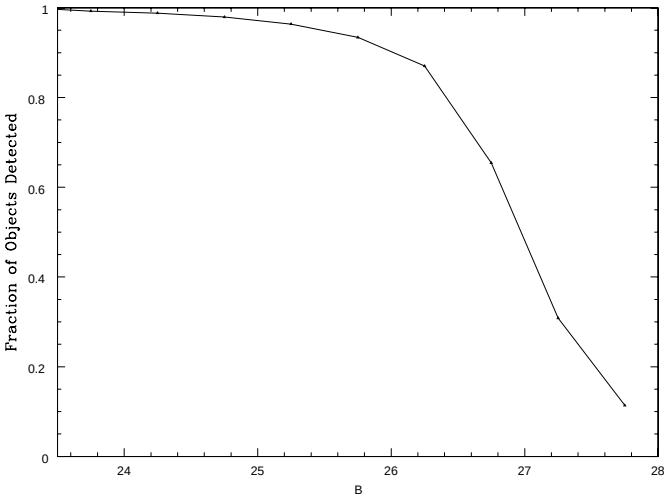

FIG. 3.—Completeness level for our photometry as a function of magnitude.

against the output magnitudes for a subsample of our artificial clusters. The dashed lines in color and magnitude indicate the input magnitude for each set of clusters.

To determine the foreground extinction and reddening in the direction of NGC 3597, we took $A_B = 0.21$ (Burstein & Heiles 1982). We then combined the extinction curve of Cardelli, Clayton, & Mathis (1989) with the filter transmission, the system response, and an A-star spectrum (which resembles that of the clusters) to calculate the extinctions. This gave $A_{\rm F450W} = 0.21$, $A_{\rm F702W} = 0.12$, and $E(450 - 702) = 0.09$.

4. RESULTS

4.1. *Photometry*

Table 1 lists the properties of all observed clusters in the PC down to a magnitude of $B = 28$, including x and y position on the chip, B magnitude, error in the magnitude, $B-R$ color, and error in the color. A color-magnitude diagram of these clusters is shown in Figure 5. A population of objects with a $B-R$ of ~ 0.7 is clearly visible. There is no clear evidence of an old globular cluster population in our images. An old cluster population, if it were similar to the Galactic globular cluster system, might be expected to have $(B-R)_0 = 1.2$ (Harris 1996), with a peak in the luminosity function at $B \sim 27$. However, detecting such a population at this magnitude is complicated both by the numerous faint objects with large errors in their colors and by rapidly increasing incompleteness. The objects that could possibly be old clusters do not even serve to put any meaningful upper limits on the number of old clusters, given the incomplete areal coverage and the unknown surface density profile of the old cluster population. The WFs have been excluded from this plot owing to the potentially large fraction of spurious objects, including foreground stars and background galaxies. A plot of $B-R$ color versus magnitude for the ~ 400 objects detected in the WFs is shown in Figure 6.

We show a color-magnitude diagram of all the objects in the PC with errors in B and R of <0.15 mag in Figure 7. This subsample of 171 objects was chosen to determine the spread in colors of the clusters to constrain possible mechanisms for cluster formation. Figure 4 shows the color spread expected from photometric errors if these clusters are a single-color, single-age population with a constant size. The color spread seen in this plot is likely to be an underestimate of the actual spread, as it does not account for errors in the aperture correction due to varying cluster sizes and variation of the PSF across the field.

TABLE 1

PHOTOMETRY FOR ALL OBSERVED CLUSTERS WITH $B > 28$

x (pixels)	y (pixels)	B	σ_B	$B-$R	σ_{B-R}
171.74.....	449.82	20.795	0.004	0.696	0.005
355.90.....	113.53	20.891	0.005	0.614	0.006
171.52.....	647.67	21.014	0.005	0.637	0.006
754.06.....	425.18	21.340	0.005	2.208	0.005
277.06.....	253.02	21.469	0.006	0.595	0.008

NOTE.—Table 1 is presented in its entirety in the electronic edition of the Astronomical Journal. A portion is shown here for guidance regarding its form and content.

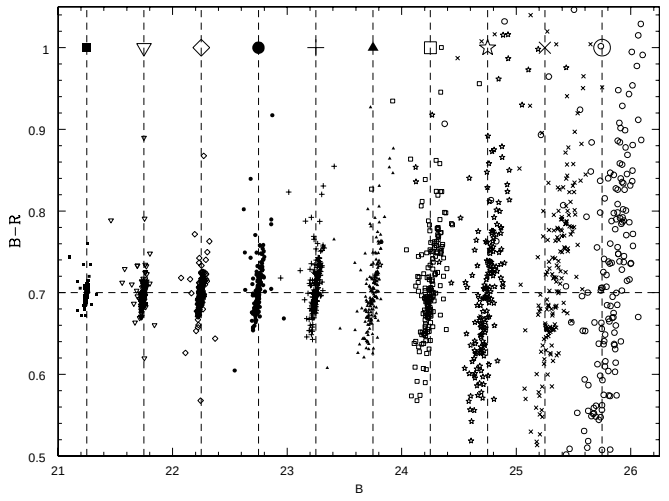

FIG. 4.—Spread in color and magnitude for a subsample of the artificial clusters from our completeness tests. The points show a slight slope at a given magnitude because an artificial cluster that is a little faint in B will appear redder, while those which are a little bright in B will appear bluer.

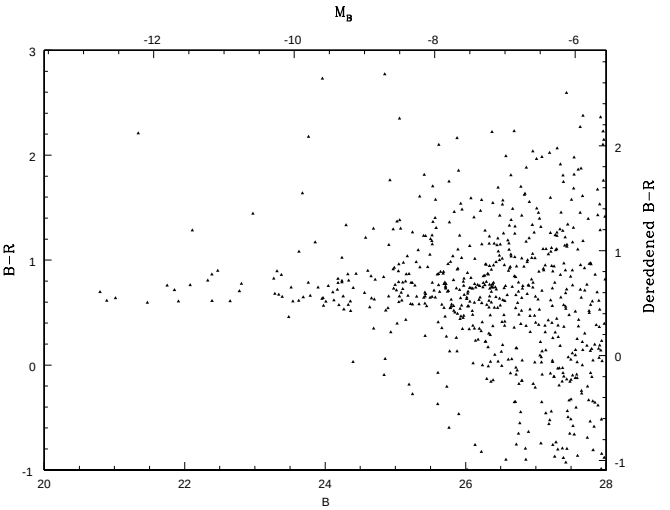

FIG. 5.—$B-R$ vs. B magnitude for all 682 objects in the PC

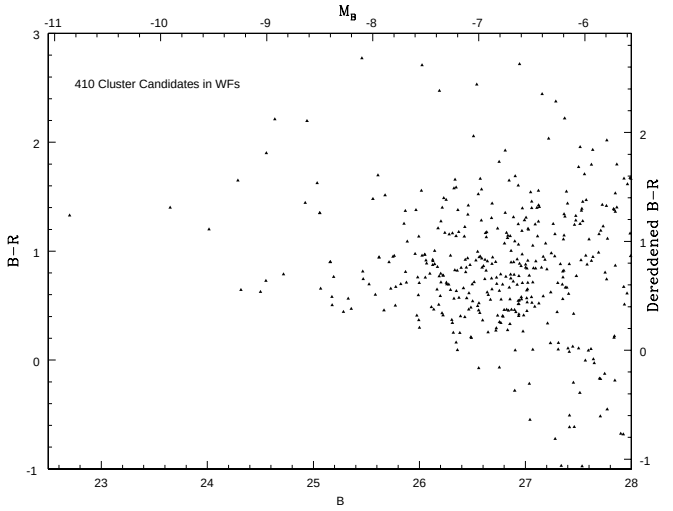

FIG. 6.—$B-R$ vs. B magnitude for the 410 objects detected in the WFs

In Figure 8, we show a histogram of the colors for the real clusters and a subsample of the artificial clusters for the B magnitude ranges <25.5, 25.5–26, 26–26.5, and 26.5–27. We have scaled the total number of clusters in the artificial cluster samples to match the total numbers of clusters in the real cluster samples. Fake clusters have been chosen randomly from our completeness tests but in the same distribution with respect to our three annuli as the real clusters. Error bars are Poisson errors in the number of real clusters. For the observed clusters, particularly for those with $B < 25.5$, there is an excess of objects redward of the peak, which is to be expected if internal differential reddening is a factor. We propose that the spread in the observed colors of the clusters in the PC is consistent with a single-color population with a spread owing to photometric errors and varying reddening within NGC 3597. If we were to assume no differential reddening, we can determine an upper limit to the age spread by measuring the color spread in the brightest clusters. This spread in $B-R$ suggests an age spread of <300 Myr.

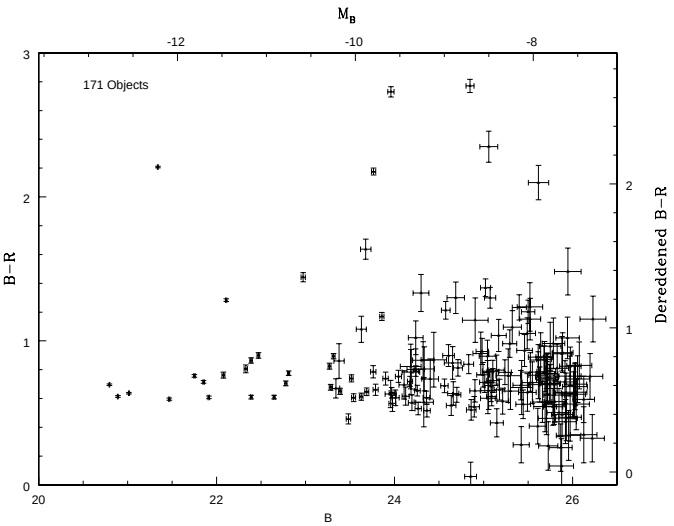

FIG. 7.—$B-R$ vs. B magnitude for all objects in the PC with errors in both B and R of <0.15 mag.

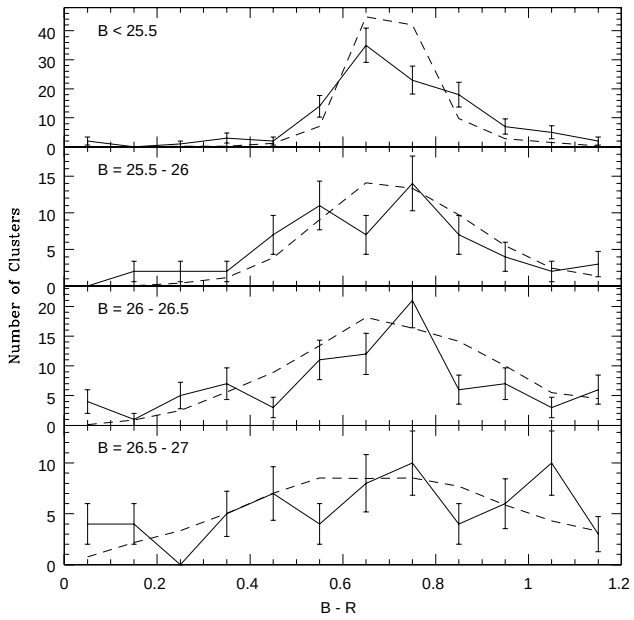

FIG. 8.—Spread in colors for different magnitude subsamples of our artificial clusters compared to the color spread of the real clusters.

The spread in color of the blue clusters can also be compared to the spread in color seen in the blue clusters in the LMC, where we can directly measure the age of the clusters. In the LMC, the spread in $B-V$ between 100 and 600 Myr is 0.2 mag, which corresponds to a spread of 0.3 mag in $B-R$, which is larger than the observed spread in NGC 3597.

We calculate the mass of the clusters by estimating their ages from their colors and then inferring the mass from the intrinsic brightness. To relate these quantities, we use the stellar population synthesis models of Charlot & Bruzual (1991). In Figure 9, we show the evolution of a single burst stellar population with a Salpeter initial mass function from

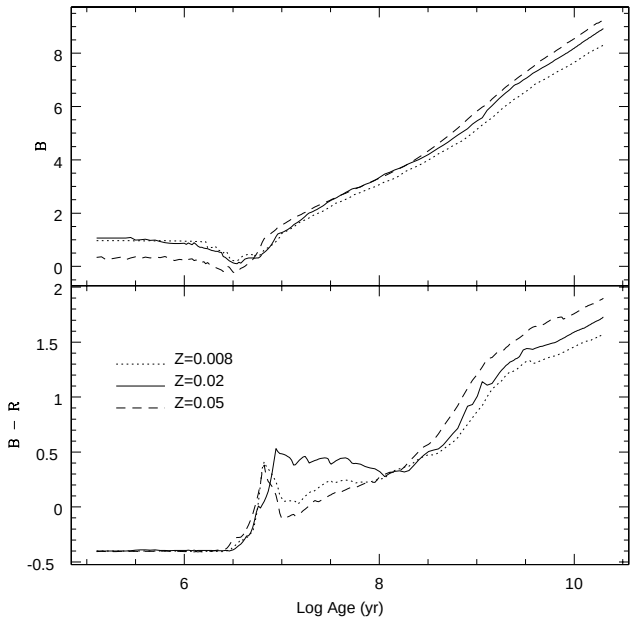

FIG. 9.—Evolution of the magnitude and color of a simple stellar population based on the models of Charlot & Bruzual (1991).

0.1 to 125 $M_\odot$, a total mass of 1 $M_\odot$, and a variety of metallicities.

Our clusters have an average $B-R \sim 0.7$. Given the Galactic reddening of 0.09, this implies a $(B-R)_0 \sim 0.6$. This suggests an age of 300–700 Myr, given uncertainties in the precise metallicity of the clusters. Therefore, the brightest cluster ($M_B = -12.8$) has an inferred mass of 5×10^6–1×10^7 $M_\odot$, which is similar to the mass of the most massive Galactic globulars. At our 50% completeness limit of $B \sim 27$ ($M_B = -6.6$), we calculate masses of 2×10^4–4×10^4 $M_\odot$.

4.2. *Luminosity Function*

We present the luminosity function for the blue clusters in NGC 3597 in Figure 10. The solid line represents actual counts of clusters. The dotted line shows the correction to the measured counts based on our completeness. Errors are simple Poisson errors in the number of counts; they do not include errors in the completeness determination, which are almost certainly the largest source of error in the last two bins of the luminosity function. The luminosity function rises to the limits of our photometry. If we approximate the luminosity function by a power law, we find $\phi(L)dL \propto L^{-2.0}$, where $\phi(L)dL$ is the number of clusters in the luminosity range of L to $L + dL$. This power-law slope is similar to those found for other blue cluster galaxies including NGC 4038/9, NGC 3921, and NGC 3256, which have best fit slopes of -1.8, -2.1, and -1.8, respectively (Whitmore & Schweizer 1995; Schweizer et al. 1996; Zepf et al. 1999).

This is distinctly different from the luminosity function of the Galactic globular cluster system, which has a roughly Gaussian magnitude distribution with a turnover at $M_B = -6.6$. If the system of blue clusters in NGC 3597 were simply a younger version of the globular cluster system of the Galaxy, we would predict a turnover in the luminosity function at $B \sim 23$. However, if we follow Zepf et al. (1999) and assume an initial power-law luminosity function for the young clusters and estimate the degree of cluster destruction through evaporation and tidal shocks, we would predict that the luminosity function of the young clusters in NGC 3597 would have a turnover at $B \approx 28$, 1 mag below our 50% completeness level. Although the present-day luminosity function of these clusters may resemble that of *open* clusters in the Galaxy, the masses, luminosities, and sizes of the individual clusters suggest that they are more closely related to Galactic globular clusters. The objects detected in the WFs have been excluded from this luminosity function.

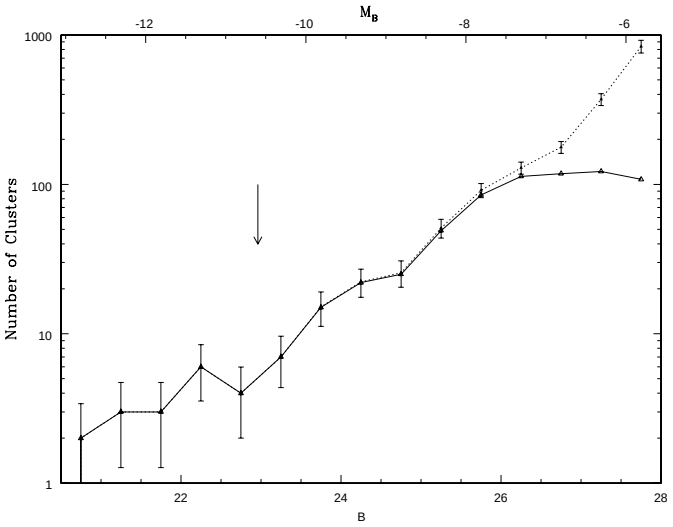

FIG. 10.—Luminosity function of all objects detected in the PC. The dotted line shows the correction for incompleteness at faint magnitudes. The arrow indicates where the turnover in the Galactic globular cluster luminosity function would be seen at an age of 500 Myr old, assuming no evolution in the shape of the luminosity function.

It has been proposed by Meurer (1995) that the increasing LF of the young clusters observed in NGC 4038/9 may come to form a Gaussian LF after 10 Gyr because of the spread in ages of the clusters. We have tested this possibility by doing a similar analysis to that of Fritze–von Alvensleben (1998), assuming that *all* of the color spread is due to spread in the ages of the clusters. We used the photometric evolution models of Charlot & Bruzual (1991) to estimate the age of each individual cluster. We then determined the magnitude change for a given cluster between the current age and the age in 13 Gyr. This information was used to create a luminosity function of the blue clusters after 13 Gyr of fading. The resultant LF is still an increasing function and does not resemble the Galactic GCLF down to 2 mag below the predicted turnover (our rough completeness limit). Based on this evidence, we suggest that while age spread effects alone may possibly explain the difference between the observed increasing luminosity function in NGC 4038/9 and a Gaussian old globular cluster luminosity function, it cannot explain this difference in NGC 3597. We suggest that age spread is likely not responsible for the discrepancy between young and old globular cluster luminosity functions in systems in which the age of the young cluster system is older than a few hundred Myr.

4.3. *Surface Density Profile*

To determine the radial surface density profile, we have taken three subsamples (all clusters with $B < 25$, <25.5, and <26) of the data from the PC and measured the surface density of clusters in each of eight different annuli. All of these subsamples are $\gtrsim 90\%$ complete, with the exception of the innermost annulus for the faintest subsample. Each annulus was 50 pixels wide, centered from 175 to 475 pixels from the center of NGC 3597. Correction has been made for incomplete areal coverage in the larger annuli. The density profile is shown in Figure 11.

Also plotted in Figure 11 is the prediction for the surface density profile of the old cluster population. This power law is derived from the power-law slope versus galaxy brightness relation of Harris (1993; see also correction of Kaisler et al. 1996). This empirical correlation is based on observations of the globular cluster systems of nearby galaxies. The predictions for the power law given the 1 σ error bars on the slope are also shown. Using $M_V = -21.18$ for NGC 3597 gives a power-law slope of -1.86. Best fits for our samples with $B < 25$, <25.5, and <26 give slopes of -1.81, -2.25, and -2.28, respectively.

Ashman & Zepf (1992) predict that the in the case of a merger, the newly formed clusters will have a density distribution that is more sharply peaked than the existing cluster population. Our data shows little deviation from the *predicted* distribution of the old clusters. Note, however, that we have no data on the actual radial surface density profile of the old cluster system.

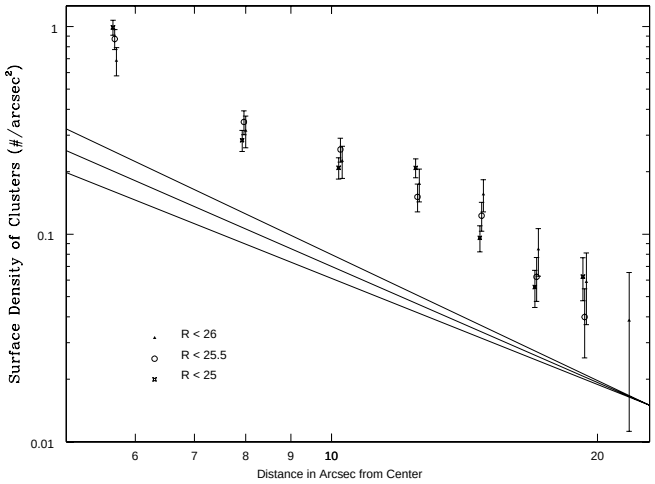

FIG. 11.—Observed surface density profile for three subsamples of the cluster candidates in NGC 3597. The solid lines show the prediction for the surface density profile of an old globular cluster population for NGC 3597 based on the empirical model of Harris (1993). Also shown are the predictions given the 1 σ error bars on the power-law slope.

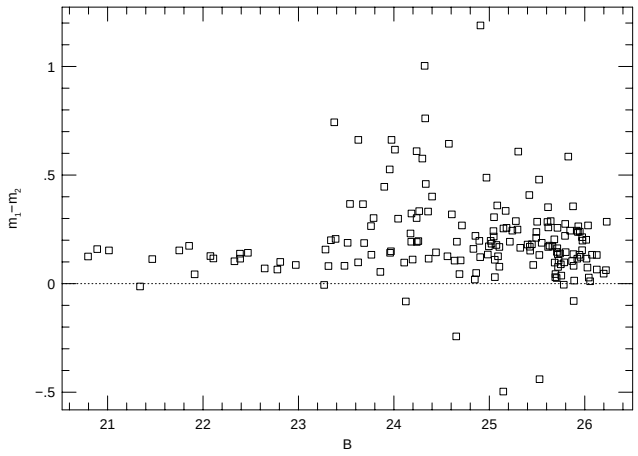

FIG. 12.—Measurements of $m_1 - m_2$ in F702W for all objects, where $m_1 - m_2$ is the difference between a 1 and 2 pixel aperture magnitude relative to the same quantity measured on a model point source. Positive values suggest that the objects are marginally resolved.

4.4. *Specific Frequency*

The specific frequency is defined as the total number of globular clusters per absolute V magnitude of -15 (Harris & van den Bergh 1981). Computing this quantity for a merger-related population can be problematic (Carlson et al. 1998). Uncertainties in the completeness and the cluster surface density profile can greatly affect the estimate of the number of clusters. The absolute V magnitude is dependent on the choice of Hubble constant and the extinction by dust, particularly within the galaxy. Estimating the future specific frequency after the population has aged is even more problematic: the total V magnitude of the galaxy in the future will depend on the ages and metallicities of the galaxy population as well as the accuracy of stellar evolution models. Determining the evolution of multiple stellar populations with poorly constrained initial conditions is a large source of potential error. The total number of clusters is also uncertain since it depends on the effectiveness of cluster destruction mechanisms.

Despite these potential complications, we can still make some estimates that may provide some limits. Even if we assume that there were *no* globular clusters associated with the progenitor spirals, we can compute a specific frequency for the galaxy based on the observed blue clusters alone. We have observed ~ 700 blue clusters, and the total V magnitude of the galaxy is $M_V = -21.18$, which gives a specific frequency of 2.4. This lower limit to the *current* specific frequency is above the typical range of specific frequency for spiral galaxies (0.5–2) and within the typical range for ellipticals (1–7). The future specific frequency is difficult to predict since it depends on the degree of galaxy fading, which would increase the specific frequency, and the extent of cluster destruction, which would decrease it.

4.5. *Sizes*

We have estimated the relative sizes of the objects in the PC images based on their 1 to 2 pixel aperture magnitude difference, $m_1 - m_2$. Following Holtzman et al. (1996), we compare this $m_1 - m_2$ for each cluster to that measured for a model PSF convolved with a modified Hubble profile placed at the same location as the cluster. Figure 12 shows the distribution of this difference in $m_1 - m_2$ between the observed and the model PSFs, plotted against the B magnitude; for the fainter objects, photometric error contributes significant spread. A value of 0 indicates an unresolved object, whereas positive values indicate the object is resolved. Figure 12 demonstrates that most of the objects appear to be slightly resolved, with typical $m_1 - m_2$ values of 0.15. The bright object at $B \sim 21.3$ that has $m_1 - m_2 \sim 0$ also is quite red (see Fig. 7), and we suggest that it is a foreground star.

If we assume that the cluster light distributions are well fitted by modified Hubble profiles, these measurements provide an estimate of the core radii of the clusters based on the model results of Holtzman et al. (1996). We estimate the core radii to be ~ 0.02–0.05 pixels, which corresponds to ~ 0.2–0.5 pc. Although there are some uncertainties in these measurements because we do not know the exact form of the cluster surface brightness distribution and because of possible errors in our assumed PSF, these objects are clearly compact, more closely resembling globular clusters than open clusters.

5. CONCLUSIONS

In deep WFPC2 observations of NGC 3597, we have detected a population of ~ 700 young blue clusters. These clusters may be a single-color, single-age population, based on our estimates of the errors in our photometry. We propose that these objects are a system of young globular clusters that formed in a single catastrophic event, the recent merger.

The luminosity function of the young clusters does not resemble the lognormal globular cluster luminosity function observed in old globular cluster systems. Instead, the luminosity function increases to the limits of our photometry. Van den Bergh (1995) uses a similar increasing luminosity function in NGC 4038/9 to argue that these objects are similar to Galactic open clusters rather than globulars. However, the high luminosities and masses of the individual clusters and their observed compactness provide compelling evidence that these clusters are more closely related to Galactic globulars. This interpretation suggests that if the system of young clusters in NGC 3597 will come to

resemble the Galactic globular cluster system, there must be evolution in the luminosity function of globular clusters on a timescale of ~ 10 Gyr that preferentially destroys fainter, less massive clusters (probably through evaporation). With our assumption of 4 mag of fading in the luminosity of the clusters over then next 13 Gyr, 95% of the currently known young clusters in NGC 3597 would have to be destroyed in that time to create a luminosity function with the same shape and turnover as that of the Galactic globular cluster system.

This work was supported in part by NASA under contract NAS 7-918 to J. P. L. and a grant to M. C. from the New Mexico Space Grant Consortium.

REFERENCES

Ashman, K. M., & Zepf, S. E. 1992, ApJ, 384, 50
Bahcall, J. N., & Soneira, R. M. 1980, ApJS, 44, 73
Burstein, D., & Heiles, C. 1982, AJ, 87, 1165
Cardelli, J. A., Clayton, G. C., & Mathis, J. S. 1989, ApJ, 345, 245
Carlson, M. N., et al. 1998, AJ, 115, 1778
Charlot, S., & Bruzual A., G. 1991, ApJ, 367, 126
de Vaucouleurs, G., de Vaucouleurs, A., Corwin, H. G., Jr., Buta, R. J., Paturel, G., & Fouque, P. 1991, Third Reference Catalogue of Bright Galaxies (New York: Springer)
Fritze–von Alvensleben, U. 1998, A&A, 336 83
Harris, W. E. 1993, in ASP Conf. Ser. 48, The Globular Cluster Galaxy Connection, ed. G. H. Smith & J. P. Brodie (San Francisco: ASP), 472
———. 1996, AJ, 112, 1487
Harris, W. E., & van den Bergh, S. 1981, AJ, 251, 497
Holtzman, J. A., et al. 1995a, PASP, 107, 156
Holtzman, J. A., et al. 1995b, PASP, 107, 1065
———. 1996, AJ, 112, 416
Kaisler, D., Harris, W. E., Crabtree, D. R., & Richer, H. B. 1996, AJ, 111, 2224
Lutz, D. 1991, A&A, 245, 31
Meurer, G. R. 1995, Nature, 375, 742
Miller, B. W., Whitmore, B. C., Schweizer, F., & Fall, S. M. 1997, AJ, 114, 2381
Schweizer, F., Miller, B. W., Whitmore, B. C., & Fall, S. M. 1996, AJ, 112, 1839
van den Bergh, S. 1995, ApJ, 450, 27
Whitmore, B. C., & Schweizer, F. 1995, AJ, 109, 960
Zepf, S. E., Ashman, K. M., English, J., Freeman, K. C., & Sharples, R. M. 1999, AJ, submitted